Characterization of flame-sprayed Al_2O_3-based coatings with a low amount of Cr_2O_3 and SiC content deposited on steels

M.Tech. Thesis

By

Neeraj Meena

DEPARTMENT OF MECHANICAL ENGINEERING

INDIAN INSTITUTE OF TECHNOLOGY INDORE

June 2025

Characterization of flame-sprayed Al_2O_3-based coatings with a low amount of Cr_2O_3 and SiC content deposited on steels

A THESIS

Submitted in partial fulfillment of the requirements for the award of the degree

of

Master of Technology

by

NEERAJ MEENA

DEPARTMENT OF MECHANICAL ENGINEERING

INDIAN INSTITUTE OF TECHNOLOGY INDORE

June 2025

INDIAN INSTITUTE OF TECHNOLOGY INDORE

CANDIDATE'S DECLARATION

I hereby certify that the work which is being presented in the thesis entitled **Characterization of flame-sprayed Al_2O_3-based coatings with a low amount of Cr_2O_3 and SiC content deposited on steels** in the partial fulfillment of the requirements for the award of the degree of **MASTER OF TECHNOLOGY** and submitted in the **DEPARTMENT OF MECHANICAL ENGINEERING Indian Institute of Technology Indore**, is an authentic record of my own work carried out during the time period from July 2023 to June 2025 under the supervision of **Prof. Kazi Sabiruddin, Professor, Department of Mechanical Engineering IIT Indore**.

The matter presented in this thesis has not been submitted by me for the award of any other degree of this or any other institute.

04/06/2025

Signature of the student with date
NEERAJ MEENA

This is to certify that the above statement made by the candidate is correct to the best of my/our knowledge.

17/6/25

Signature of the Supervisor of M.Tech. thesis (with date)
Prof. Kazi Sabiruddin

Neeraj Meena has successfully given his/her M.Tech. Oral Examination held on **26 May 2025**.

Signature(s) of Supervisor(s) of M.Tech. thesis
Date: **17/6/25**

Convener, DPGC
Date:17-06-25

ACKNOWLEDGEMENTS

I, Neeraj Meena, express my heartfelt gratitude to all those who have contributed to the successful completion of my M.Tech. thesis in Advanced Manufacturing.

I am deeply thankful to my supervisor, Prof. Kazi Sabiruddin Sir, for his invaluable guidance, encouragement, and unwavering support throughout this journey. His expertise and insights have been instrumental in shaping this work.

I extend my sincere appreciation to my lab seniors, Setu Suman, Manish Kumar, and Ashok Kumar, for their constant support, technical assistance, and motivation, which greatly enriched my research experience.

I am also grateful to my lab junior, Himanshu Singh, for his dedicated support in the project work. His contributions have been vital, and I wish him the very best as he continues this project further. My heartfelt thanks go to my friends and family for their unconditional love, encouragement, and motivation, which kept me focused and determined throughout this endeavor.

I also acknowledge the support provided by the college facilities, which played a crucial role in facilitating my project work. Thank you all for being an integral part of this journey.

Regards,

Neeraj Meena

Abstract

This study explores the use of the flame spray technique to deposit alumina-based coatings enhanced with small additions of chromia (Cr_2O_3) and silicon carbide (SiC). Alumina is widely recognized for its high thermal resistance and durability, and the incorporation of limited amounts of Cr_2O_3 and SiC is intended to improve its overall mechanical and protective properties. Coatings were applied to metallic substrates using flame spraying, and the resulting layers were examined for structural integrity, surface morphology, phase composition, hardness, and adhesion. The experimental results show that even low concentrations (≤10 wt.%) of Cr_2O_3 and SiC contribute to better hardness and thermal performance, while maintaining low porosity and strong bonding with the substrate. The findings suggest that these composite coatings could be suitable for industrial applications requiring resistance to wear and high temperatures, offering a cost-effective and efficient surface modification approach.

TABLE OF CONTENTS

Chapter 1

Chapter 2

Chapter 3

LIST OF FIGURES

LIST OF TABLES

Chapter 1

Introduction

1.1 Surface Engineering

Surface engineering is a multidisciplinary field that involves the design and modification of surface properties of materials to meet specific functional requirements. It bridges materials science, mechanical engineering, and chemistry to solve surface-related problems in a wide array of applications. The surface of a component often serves as the primary interface with its environment and is subjected to various stresses, including mechanical wear, chemical attack, thermal fluctuations, and fatigue. These stresses can lead to premature failure if not properly managed.

By altering the surface without necessarily changing the bulk properties of the material surface engineering allows for enhanced performance, durability, and cost efficiency. Common surface properties targeted for improvement include hardness, friction, corrosion resistance, thermal conductivity, and resistance to erosion or oxidation. Techniques in surface engineering range from physical and chemical treatments, such as carburizing, nitriding, and ion implantation, to coating methods like electroplating, physical vapor deposition (PVD), chemical vapor deposition (CVD), and thermal spraying.

This field plays a pivotal role in high-performance industries such as aerospace, automotive, energy, biomedical, and manufacturing. For example, in aerospace, turbine blades are coated to resist high-temperature oxidation and wear, whereas in biomedical implants, surface modifications improve biocompatibility and reduce wear against bone or tissue. As industries push the limits of material performance, surface engineering becomes increasingly essential in optimizing functionality while minimizing maintenance and costs.

1.2 Thermal Spray Coatings

Thermal spray coating is a well-established surface engineering process used to deposit a wide range of materials—metals, alloys, ceramics, polymers, and composites—onto substrates to improve their surface characteristics. It is a family of processes where the feedstock material is heated to a molten or semi-molten state and then accelerated towards the surface to be coated. Upon impact, the particles flatten and rapidly solidify, forming a protective or functional-layer.

There are several variants of thermal spray processes, including flame spraying, plasma spraying, electric arc spraying, high-velocity oxy-fuel (HVOF), and cold spraying. Each method differs primarily in the energy source used to melt the material and the velocity of particle propulsion. The selection of a suitable method depends on the substrate material, coating material, application environment, and the required coating performance.

Thermal spray coatings offer a unique advantage in that they do not require the substrate to be melted, minimizing thermal distortion or degradation of the base material. This allows thermal spray processes to be used on temperature-sensitive components or finished parts with tight dimensional tolerances. Additionally, coatings can be applied relatively thick—ranging from micrometers to several millimeters—enabling both wear protection and dimensional-restoration.

Thermal spraying is extensively used in both preventive and corrective maintenance. Applications include hard-facing of tools, thermal barrier coatings on turbine components, corrosion-resistant coatings in offshore structures, electrical insulation or conductivity enhancement in electronic parts, and biomedical coatings for implants. Its flexibility and adaptability to a wide variety of materials and geometries make it one of the most widely adopted coating technologies in modern industry.

1.3 Flame Spray Coatings

Flame spraying is one of the earliest and most accessible thermal spray techniques, widely used due to its simplicity, portability, and relatively low operational cost. The process utilizes a flame produced by the combustion of fuel gases—typically acetylene, propane, or hydrogen—with oxygen to heat the coating material.

This feedstock, usually in the form of powder or wire, is melted or softened in the flame and then propelled onto the target surface using a stream of compressed air or another carrier gas.

The molten or semi-molten particles impact the surface, flatten, and solidify rapidly to form a continuous coating. Despite being less technologically advanced than plasma or HVOF spraying, flame spray coatings are widely used in maintenance, repair, and overhaul (MRO) settings due to the ease of operation and equipment mobility. It is especially advantageous for coating large components or in-field repairs, where high-end equipment may be impractical to deploy.

However, the relatively lower particle velocity and temperature in flame spraying compared to other methods result in coatings that may have higher porosity and weaker adhesion to the substrate. These limitations can affect the coating's resistance to wear, corrosion, and fatigue. Nevertheless, advances in feedstock materials and process control have improved the quality of flame-sprayed coatings. For many applications, particularly where high precision is not critical, flame spraying provides a good balance between performance and cost-effectiveness.

Flame spraying is used in a variety of industries. Examples include applying wear-resistant layers on shafts and rollers, corrosion-resistant coatings on pipelines and marine structures, and thermal insulation coatings on industrial furnace components. The method's

ability to coat large, irregular surfaces without extensive pre- or post-treatment makes it a practical choice for many real-world applications.

1.4 Coating Materials

The selection of appropriate coating materials is central to the success of surface engineering via thermal spraying. Coatings must be tailored to the operational demands of the component, considering factors such as mechanical load, thermal exposure, chemical environment, and required lifespan. Among the vast range of materials used, ceramics stand out for their exceptional hardness, chemical stability, and resistance to thermal and electrical conduction.

Alumina (Al_2O_3) is one of the most commonly used ceramic materials in thermal spraying. It offers excellent wear resistance, high dielectric strength, and outstanding stability at elevated temperatures. Coatings of alumina are often applied to components subjected to abrasive wear or requiring electrical insulation, such as printing rollers, electrical insulators, and pump seals.
To further enhance performance, alumina can be combined with other oxides or compounds. Chromia (Cr_2O_3) is frequently added to improve corrosion resistance, particularly in acidic or oxidative environments. Its low solubility in most corrosive agents and ability to form a stable passive layer make it ideal for chemical processing and marine applications. Silicon carbide (SiC), another important

additive, provides high thermal conductivity and mechanical reinforcement. SiC's ability to withstand high temperatures while maintaining structural integrity makes it suitable for applications such as heat exchangers, engine components, and aerospace shielding.

Beyond ceramics, metallic and cermet coatings are also widely used. These include tungsten carbide-cobalt (WC-Co) for extreme wear resistance, nickel-based alloys for corrosion protection, and molybdenum for lubrication and anti-galling. The versatility of thermal spray processes allows these materials to be applied individually or as composites, offering a tailored solution for nearly any engineering surface requirement. Material selection also considers the compatibility between the coating and substrate to prevent delamination or cracking. Advanced characterization techniques—such as scanning electron microscopy (SEM), X-ray diffraction (XRD), and thermal cycling tests—are used to assess coating integrity, phase composition, and performance under service conditions. The future of coating materials lies in smart and multifunctional materials capable of self-healing, real-time monitoring, or adaptive performance, making this an active and evolving field of research.

Chapter 2

Literature Survey

2.1 Overview

Advanced ceramic coatings have become crucial for improving the surface characteristics of engineering components used in industries such as aerospace, automotive, energy, and chemical processing. Among the various ceramic coatings available, alumina (Al_2O_3) stands out due to its outstanding hardness, resistance to wear, electrical insulation properties, and thermal stability. Nevertheless, alumina's inherent brittleness, tendency to undergo phase changes under thermal stress, and limited toughness have motivated researchers to enhance it by adding secondary phases like chromia (Cr_2O_3) and silicon carbide (SiC). Even small amounts of these reinforcements can greatly enhance the mechanical strength, thermal stability, and abrasion resistance of the coatings.

Thermal spray methods, including plasma spraying, high-velocity oxy-fuel (HVOF), and flame spraying, have gained popularity as effective ways to deposit these ceramic coatings. Flame spraying, in particular, is valued for its cost-efficiency, operational simplicity, and suitability for large-scale or on-site applications. This process supports the coating of a wide variety of materials, including metal-ceramic composites and oxide blends. Although flame spraying typically results in coatings with higher porosity compared to plasma spraying, recent developments have improved control over microstructure, phase preservation, and coating adhesion.

Incorporating small amounts of chromia and SiC into alumina coatings via flame spraying offers distinct benefits. Chromia helps increase hardness and stabilizes the α-alumina phase (corundum), which is desirable for its mechanical properties. Meanwhile, SiC contributes to enhanced toughness and improved wear resistance. Achieving these benefits at low additive concentrations demands precise management of powder preparation, spraying parameters, and post-processing to ensure uniform distribution and strong bonding of the additives within the alumina matrix.

This review integrates recent research findings concerning flame-sprayed alumina coatings with limited chromia and SiC content, highlighting current knowledge, challenges, and potential areas for further study in surface engineering.

2.2 Background

Ceramic coatings are widely employed to provide wear resistance, thermal protection, and corrosion defence in demanding environments. Alumina is often selected for such applications due to its high melting temperature, chemical stability, and favourable mechanical attributes. However, the performance of alumina coatings largely depends on their crystalline phase composition. The α-phase is the most desirable form because of its superior hardness and thermal resistance. Rapid solidification during thermal spraying, however, frequently results in metastable phases like γ- and δ-alumina, which can detract from the coating's properties. Therefore, additives such as Cr_2O_3 and SiC are incorporated to

promote α-phase retention and overall enhancement of coating characteristics.

Key findings from the literature include:

- Balmukund Dhakar showed that mechanically blending alumina with controlled amounts of chromia leads to improved stabilization of the α-phase when coatings are deposited by plasma spraying, which enhances hardness, density, and thermal stability.
- Tomas Tesar utilized hybrid suspension plasma spray techniques to fabricate alumina-chromia coatings with increased α-phase content by exploring different feedstock mixing methods to control microstructure.
- K.A. Habib's investigation into flame-sprayed NiCrBSi coatings revealed that smaller alumina particles produce denser coatings with superior mechanical properties and wear resistance, underscoring the importance of particle size and distribution in composite systems.
- Research by Vishal Sharma and Kazi Sabiruddin demonstrated that incorporating SiC in Al_2O_3 coatings using detonation gun spraying substantially improves erosion resistance, an effect relevant for flame-sprayed coatings with lower SiC amounts.
- Hipolito Carvajal's study on NiCrSiBFeC/SiC composite coatings via flame spraying reported significant enhancement in abrasion resistance even with moderate SiC additions, confirming SiC's role in long-term durability.

- Geng Sheng Lin's work on silica gel-coated SiC layers produced by atmospheric plasma spraying, although not flame-sprayed, offers insights into coating adhesion and phase integrity applicable to similar composite systems.

- A. Nistal addressed challenges in flame spraying silicon onto SiC substrates, highlighting issues in achieving uniform coating and strong adhesion, which is important for multi-material compatibility.

- S. Conze and M. Grimm's study on alumina coatings with Cr_2O_3 and TiO_2 additions through APS indicated that synergistic effects of additives influence porosity, microstructure, and wear performance, stressing the need for precise multi-phase coating control.

  Collectively, these studies emphasize the critical role of additive selection, particle morphology, feedstock preparation, and process optimization in producing alumina-based coatings with enhanced performance. While extensive research exists for high additive concentrations and other thermal spray methods, systematic investigations on alumina coatings with low chromia and SiC additions deposited by flame spraying are limited. This reveals a distinct research gap regarding how minimal amounts of these additives affect the microstructure and functional properties of flame-sprayed alumina coatings.

2.3 Research Objectives

This study aims to develop and characterize alumina-based coatings containing less than 10 wt.% of chromia (Cr_2O_3) and silicon carbide (SiC), applied through the flame spray technique. The primary goal is to understand how such minor additions influence the microstructure, phase stability, wear resistance, and internal cohesion of the coatings. Comprehensive characterization methods including scanning electron microscopy (SEM), wear testing, X-ray diffraction (XRD), and cross-sectional analysis will be employed to elucidate the relationships between processing, structure, and properties.

Key focus areas include:

- **SEM Morphology Analysis**: Investigate the surface topography, splat formation, porosity, and bonding between particles. Assess how Cr_2O_3 and SiC additives affect melting behaviour, adhesion, and porosity levels. Use energy-dispersive spectroscopy (EDS) to verify uniform additive distribution within the alumina matrix.
- **Wear Behaviour Evaluation**: Conduct abrasive and sliding wear tests (e.g., pin-on-disc) under standardized conditions. Measure parameters such as wear rate, volume loss, and friction coefficient. Correlate wear performance with additive presence and distribution. Analyse worn surfaces via SEM to identify wear mechanisms.

- **XRD Phase Characterization**: Determine the phase composition, focusing on the α- to γ-alumina ratio. Evaluate how chromia promotes α-phase stabilization and how SiC influences thermal response. Detect any secondary phases arising from chemical interactions. Relate crystallographic data to hardness and wear resistance.

- **Cross-Sectional Analysis**: Use SEM and optical microscopy to examine coating thickness, interface bonding quality, and defect occurrence. Evaluate the structural integrity of the coating-substrate interface. Study the effects of additives on internal porosity, microcracking, and adhesion strength.

  Together, these objectives aim to clarify how flame spray parameters and low-level additive incorporation affect coating performance. The ultimate goal is to develop durable, mechanically robust alumina coatings while maintaining cost-effectiveness and scalability for industrial use. Findings from this research will inform optimization of feedstock design and spraying processes for advanced alumina-based protective coating.

Chapter 3

Materials and Methods

3.1 Material selection

3.1.1 Steel substrate

Mild steel plates were utilized as substrates for the deposition of flame-sprayed coatings composed mainly of aluminum oxide with small additions of chromium oxide and silicon carbide. The steel was procured from (supplier name) and machined into specimens measuring 30 mm by 30 mm with a thickness of 5 mm. The chemical composition of the mild steel is shown in table:

Table 3.1 Elemental composition of AISI 1020 Steel

Elements	C	Mn	S	P	Fe
Weight%	0.16-0.23	0.3-0.6	≤ 0.05	≤ 0.04	Balance

Prior to coating application, the substrate surfaces were carefully prepared to optimize coating adherence and surface quality through a multi-step process involving mechanical grinding, suction blasting, and ultrasonic cleaning.

3.1.2 Coating material

The feedstock powder mixture comprised predominantly Nickel-5wt% alumina used as bond coat layer of the coatings and the high-

purity aluminum oxide (Al_2O_3), supplemented with low concentrations of chromium oxide (Cr_2O_3) and silicon carbide (SiC) as topcoat. Powders were sourced from (supplier name) and characterized by the following properties:

- Al_2O_3: Purity exceeding 99.5%, particle size distribution between 15 and 45 micrometers, irregular particle shape.
- Cr_2O_3: Purity above 99.0%, with particle sizes ranging from 10 to 30 micrometers, generally spherical morphology.
- SiC: Purity around 98.5%, particle sizes between 10 and 40 micrometers, angular in shape.

  Powder components were blended thoroughly in the desired proportions (maintaining Cr_2O_3 and SiC contents below 5 weight percent) using a mechanical shaker for two hours to ensure homogeneity before the spraying process.

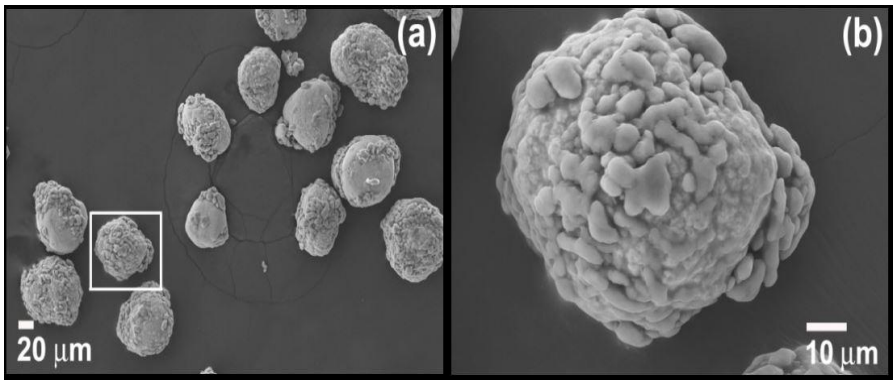

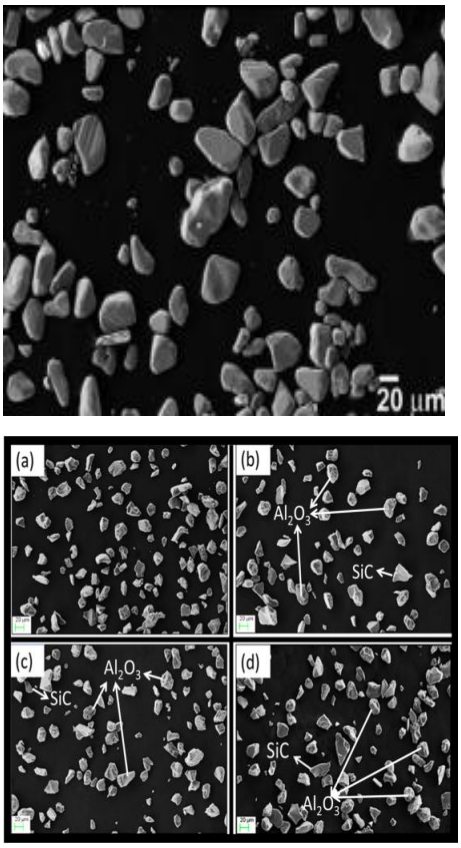

Figure 3.1 FESEM micrograph Pure Al_2O_3, Al_2O_3-Cr_2O_3 and Al_2O_3-SiC powder

3.2 Substrate Preparation

Some of the techniques required to prepare the substrate before the coating process are necessary to ensure good coating results and to achieve mechanical properties. The substrate preparation technique involves blasting, cleaning, and preheating. By performing these techniques, the mechanical interlocking between the substrate and the feedstock material becomes good and provides good adhesion

strength and other thermal properties. Sufficient dimensions, a cleaned surface, and necessary surface roughness are required to achieve good coating results.

3.2.1 Suction Blasting

Suction blasting with alumina particles sized 18 mesh to further enhance surface roughness and remove residual contaminants. The blasting was performed at a pressure of 0.5 megapascals, with the nozzle maintained about 100 millimeters from the substrate surface. Surface profilometry revealed roughness values (Ra) between 5 and 7 micrometers, optimal for mechanical interlocking of the coating.

Figure 3.2 Suction Blasting Chamber

3.2.2 Ultrasonic Cleaning

Ultrasonic cleaning utilizes high-frequency sound waves to remove loose particles from a surface while immersed in inorganic solvents such as isopropyl alcohol or acetone. These inaudible sound waves are produced in the fluid medium and eliminate impurities from all surfaces when the fluid contacts the surface. After the grit blasting, ultrasonic cleaning is performed to ensure complete removal of dust and blasting media.

Figure 3.3 Ultrasonic Cleaner

The substrates were immersed in an ultrasonic bath containing acetone and cleaned for 15 minutes at 40 kHz frequency and 200 watts power

3.2.3 Preheating the powders

We preheat the powder in the muffle furnace for 15 min at 100 ºC to ensure mechanical anchorage**.** And stop the furnace and cool down the furnace itself.

Powder feeder**:** There are so many parameters that we can change, like carrier gas, disk rpm, and flow rate. We set the powder feed rate at 4 gm/second

Carrier gas**:** We use compressed atmospheric gas as carrier gas.

3.3 Experimental setup

There is a chamber un which there is holding attachment in that chamber by which we can change the sod and height as well. The coating setup used to obtain for desired samples is shown in the figure. Using an oxy-acetylene flame spraying system (MEC), the coatings are obtained.

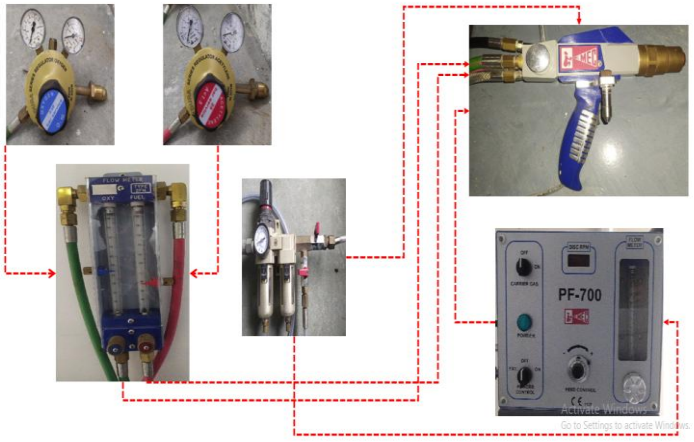

(a)

(b)

Figure 3.4 Flame spray coating setup **(a)** flame generator & **(b)** Manipulator

Compressed air is used as carrier gas, and an oxygen-acetylene mixture is used to generate a flame to melt the feedstock powder.

Manipulator: There is 2-axis manipulator shown in Figure 4(b), which is run by two stepper motors controlled by a joystick arrangement. We can change the speed of these motors to maintain uniformity in the coating. On the front side of this, there is a cantilever arrangement in which a flame spray torch is mounted. This torch is manipulated by the joystick.

Spraying parameters are used and maintained as follows:

- Oxygen flow rate: 24 liters per minute
- Acetylene flow rate: 35 liters per minute
- Powder feed rate: 3-4 grams per minute
- Carrier gas pressure: 0.3 megapascals
- Spray distance: 80 millimeters
- Traverse speed of spray gun: 100 millimeters per second
- Number of passes: 15, targeting a coating thickness of 300 micrometers

The gas flow rates were controlled to maintain a neutral to slightly oxidizing flame to prevent unwanted phase changes in the powders during deposition.

Deposition Process

Firstly, switch on the fuel gas and generate the flame than open carrier gas now open switch on the powder now we can see the color of the flame and then by joystick we move the torch on the sample for 15 passes for achieve desired thickness now same for the topcoat Substrates were preheated to approximately 100°C before coating to minimize thermal stress and enhance coating adhesion. The powder mixture was continuously fed into the flame, where particles were heated to a molten or semi-molten state and propelled onto the substrate surface. Multiple passes

were conducted to build up the desired coating thickness, ensuring uniform coverage and bonding.

All spraying operations were conducted under controlled laboratory conditions, maintaining room temperature (~22°C) and relative humidity (~50%) to ensure process repeatability.

3.4 Characterization Techniques

3.4.1 Morphology and Microstructure

Sample coatings sectioned using a high-speed cutter and then mounted through cold mounting process with the help of hardener and resin. To achieve the good view sectioned samples are polished on SiC papers with the range of 200 to 2000 mesh size, followed by diamond polishing through diamond paste of 1 µm grit size. Topology and cross-sectional microstructure are evaluated in Field Emission Scanning Electron Microscopy (FESEM).

(a)

(b)

Figure 3.5. **(a)** Polishing Machine & **(b)** Optical microscope

3.4.2 Phase Composition

Phase identification was carried out using X-ray diffraction (XRD) with X'Pert highscore diffractometer and Cu Kα radiation (λ = 1.5406 Å). Diffraction data were collected in the 2θ range from 20° to 90°, with a step size of 0.02° and a dwell time of 1 second per step.

The diffraction patterns were compared against standard JCPDS files to identify α-Al_2O_3 (corundum), Cr_2O_3, SiC, and any additional phases resulting from the spraying process.

3.4.3 Surface Roughness and Coating Thickness

Surface roughness was measured using a Taylor Hobson profilometer at five random points on each sample, providing an average Ra value. Coating thickness was measured from SEM cross-sectional images, with multiple measurements taken across the sample to calculate an average thickness, targeted around 300 ± 20 micrometers.

Figure 3.6 Surface profilometer

3.4.4 Porosity Analysis

Porosity was quantified by image analysis of the SEM top surface using ImageJ software. Thresholding techniques differentiated pores from the coating matrix, and porosity was expressed as the percentage of pore area relative to the total analyzed area. Ten images per sample were analyzed for statistical significance.

3.4.5 Wear Testing

Wear resistance was evaluated using a Linear reciprocating wear tribometer under dry sliding conditions. A hardened Tungsten carbide counter-body (5 mm diameter) was loaded with 10 N normal force against the coating surface, sliding at 0.1 m/s for a total distance of 1000 meters.

Wear scars were examined by SEM to identify wear mechanisms, and volumetric wear loss was calculated via profilometry.

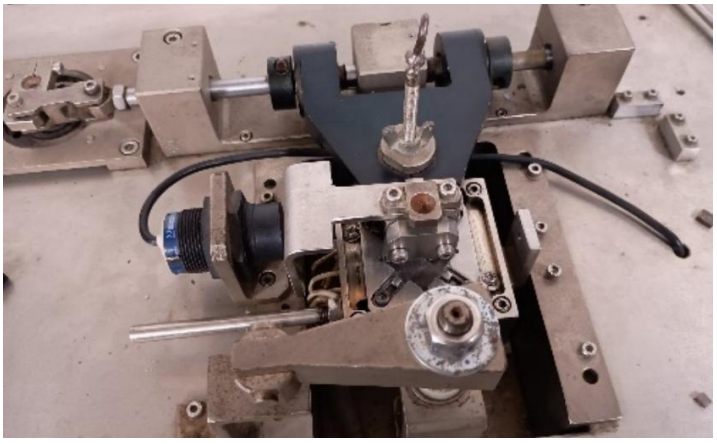

Figure 3.7 Fretting Wear tribometer (CM9104)

Chapter 4

Results and Discussion

4.1 SEM morphology

SEM of the coating displays different types of features, such as pores, voids, cracks, melted and partially melted particles in the top surface of the coating. Due to the pores, voids, and unmelted particles, porosity increases.

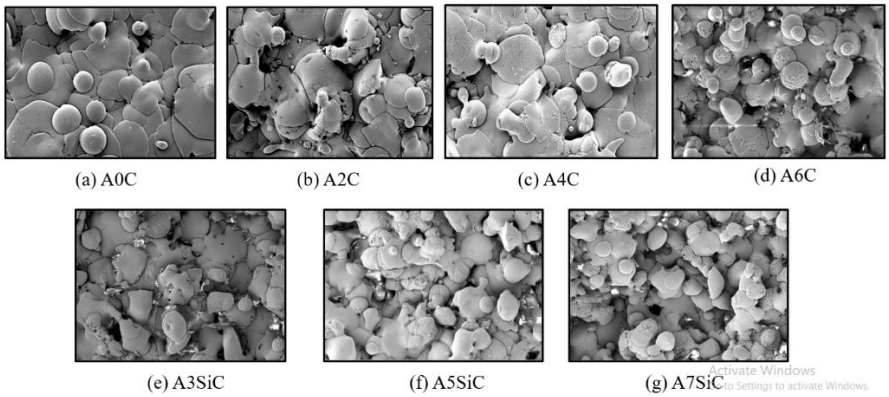

Figure 4.1 Surface morphology of Alumina-Chromia coatings and Alumina-SiC coatings

The SEM images show the surface morphology of thermally sprayed alumina-based coatings with varying amounts of Cr_2O_3 and SiC. In the A0C sample, which is pure alumina, the surface appears relatively uniform with spherical and flattened splats, indicating decent melting and deposition, though some pores and cracks are visible. With the addition of 2% Cr_2O_3 in A2C, the splat structure becomes more irregular, but there is improved packing and fewer

visible voids, suggesting enhanced densification. At 4% Cr_2O_3 in A4C, the morphology shows the best densification, with minimal porosity and well-bonded splats, indicating that this is the optimal Cr_2O_3 content. However, when the Cr_2O_3 content increases to 6% in A6C, the surface becomes rougher and more porous, with more unmelted or poorly bonded particles, likely due to additive agglomeration or phase mismatch. In the SiC series, A3SiC with 3% SiC displays a relatively compact and smooth structure with well-bonded particles and fewer voids, indicating an effective reinforcement level. With 5% SiC in A5SiC, porosity starts to increase, and the splats appear more heterogeneous and coarser, suggesting some agglomeration or reduced melting efficiency. At 7% SiC in A7SiC, the surface becomes more irregular and porous, with evident gaps and loosely bonded particles, which implies that excessive SiC content impairs coating quality due to poor dispersion and bonding. Overall, the optimal microstructure with the lowest porosity is observed at 4% Cr_2O_3 and 3% SiC. Exceeding these levels leads to increased porosity and structural degradation due to poor splat formation, particle agglomeration, and insufficient melting or bonding.

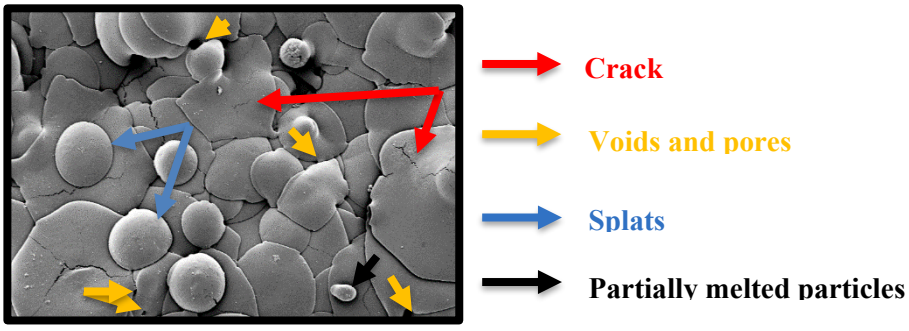

Figure 4.2. Different Surface features of the coatings

Figure 8 is an SEM image that displays a typical top surface morphology of a thermally sprayed ceramic coating, likely alumina-based. The surface is composed of overlapping and well-formed splats, which are characteristic of molten or semi-molten particles that have flattened upon impact. The blue arrows indicate these rounded, disk-like splats that suggest good melting and deposition behavior during the spray process. There are also distinct inter-splat boundaries and some visible pores or voids between splats, marked by yellow arrows, which can be due to incomplete filling or insufficient particle overlap.

Cracks are observed throughout the surface, as marked by red arrows, running along splat boundaries or through the splats themselves. These cracks likely arise from thermal stresses during rapid cooling and solidification, as well as from residual stress accumulation. The black arrow highlights a small, likely unmelted or partially melted particle embedded in the matrix, indicating that not all feedstock particles experienced complete melting. This can affect coating uniformity and mechanical strength. The overall surface reveals a dense coating with some porosity and cracking, typical of plasma-sprayed ceramic coatings, where particle melting, flattening, and solidification all influence the final microstructure**.**

4.2 Cross-sectional analysis:

The SEM micrograph of the cross-section of flame-sprayed Al2O3-based coatings is depicted in Figure. SEM coating shows a typical

layered structure, consisting of a bond coat next to the substrate and a top coat atop it.

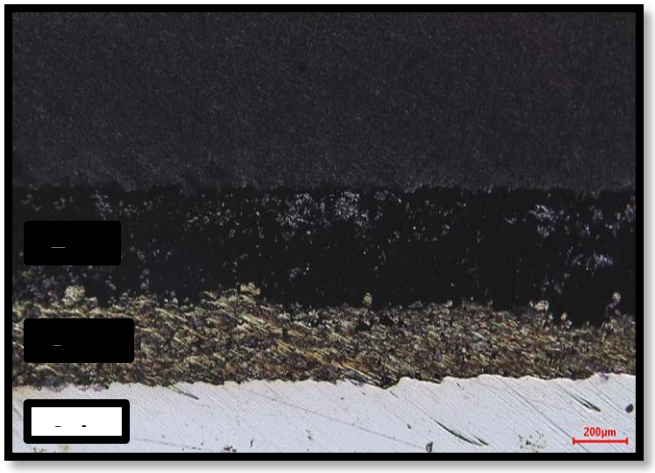

Figure 4.3 Cross-section of the coatings

This cross-sectional micrograph represents a typical thermal spray-coated system designed for enhanced surface performance under high wear, thermal, or corrosive environments. The coating consists of three distinct layers: the topcoat (blackish), the bond coat (yellowish), and the substrate (white).

The topcoat, shown as the blackish uppermost layer, is composed of Alumina–Chromia (Al_2O_3–Cr_2O_3) or Alumina–SiC (Al_2O_3–SiC) composite powder. This layer appears dense with some visible texture, suggesting a thermally sprayed ceramic coating. In the case of Alumina–Chromia, the Cr_2O_3 addition improves hardness, wear resistance, and corrosion stability due to its chemical inertness. If Alumina–SiC is used, the SiC enhances thermal conductivity and erosion resistance while maintaining a ceramic hardness. The dark contrast in the image typically represents the ceramic nature of the

material, which absorbs more light under optical microscopy. Beneath the topcoat is the bond coat, identified by its yellowish tone. This is a Nickel-5 wt. % Alumina composite layer, applied to promote adhesion between the ceramic topcoat and the metallic substrate. The addition of a small amount of alumina within the nickel matrix helps to enhance the thermal stability and wear resistance of the bond coat, while still providing ductility and metallic bonding capability. The structure appears rough and interlocked with the topcoat, suggesting good mechanical anchoring—a critical feature for layered coatings subjected to thermal cycling or mechanical stresses.

The substrate at the bottom is mild steel, visible as a white, polished region. It serves as the structural base of the coated component. The smooth interface between the substrate and the bond coat, with minimal visible delamination, indicates good metallurgical compatibility and proper deposition parameters.

Overall, the microstructure shows a well-adhered and layered thermal spray system. The integrity of the interfaces, especially the rough topcoat–bond coat interface, indicates good coating performance potential. The combination of ceramic topcoat, composite bond coat, and metallic substrate is well-suited for applications requiring resistance to high temperatures, wear, and corrosion. The coating thickness appears uniform, and the absence of major voids or cracks supports the coating's quality and durability.

4.3 Porosity analysis:

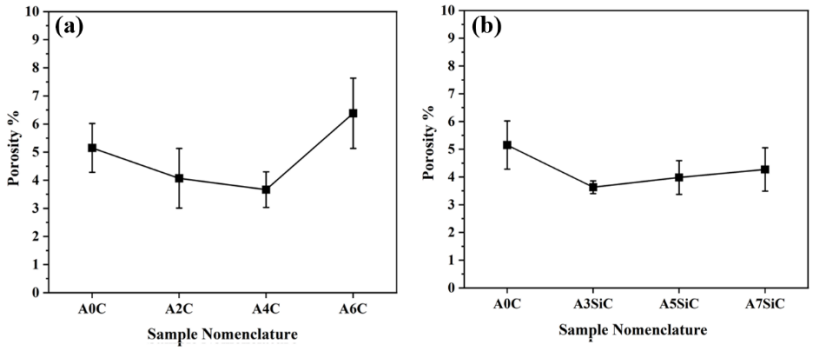

Figure 4.4 Porosity plot of Al_2O_3-Cr_2O_3 coatings and Al_2O_3-SiC coatings

This figure shows two graphs comparing the porosity (%) of different coatings:

In alumina-chromia coatings, adding Cr_2O_3 initially reduces porosity, possibly due to better particle packing or enhanced sintering. Beyond 4% Cr_2O_3, porosity increases again, likely due to agglomeration, poor dispersion, or mismatched thermal properties causing microcracks.

In Alumina–SiC Coatings, SiC addition up to 3% reduces porosity, likely by improving densification or acting as a filler. Beyond 3% SiC, porosity slightly rises, perhaps due to SiC particle clustering or limited sintering compatibility with alumina.

Both Cr_2O_3 and SiC additions improve coating density up to a threshold.

Optimal porosity reduction:

Cr_2O_3: Best at 4% (A4C)

SiC: Best at 3% (A3SiC)

Excessive additive content leads to increased porosity, likely from processing defects or poor phase integration

4.4 XRD analysis:

X-ray diffraction analysis of Al_2O_3 powder and different Al_2O_3 coatings are carried out to identify the various phases present in the powder and the coatings. The XRD patterns of four different samples labeled A0C, A2C, A4C, and A6C were analyzed to identify the crystalline phases present. The key phases are indexed as follows:

α (Alpha-alumina, Al_2O_3): Stable phase of alumina

γ (Gamma-alumina, γ-Al_2O_3): Metastable phase of alumina

Ψ (Chromium (III) oxide, Cr_2O_3)

Ω (Chromium (II) oxide, CrO)

O: $Al_{1.98}Cr_{0.02}O_3$ (Cr-substituted alumina solid solution)

Sample A0C shows dominant peaks of α-Al_2O_3, indicating a highly crystalline and stable phase. Minor peaks of γ-Al_2O_3, suggesting

partial retention of the metastable phase due to processing conditions.

No chromium-related phases are detected, as expected.

Table 4.1: Compound Nomenclature

Element	Al_2O_3	$(Al_2O_3)_{1.33}$	Cr_2O_3	CrO	$Al_{1.98}Cr_{0.02}O_3$	Si	C	SiC
Nomenclature	α	γ	Ψ	Ω	O	•	*	♦

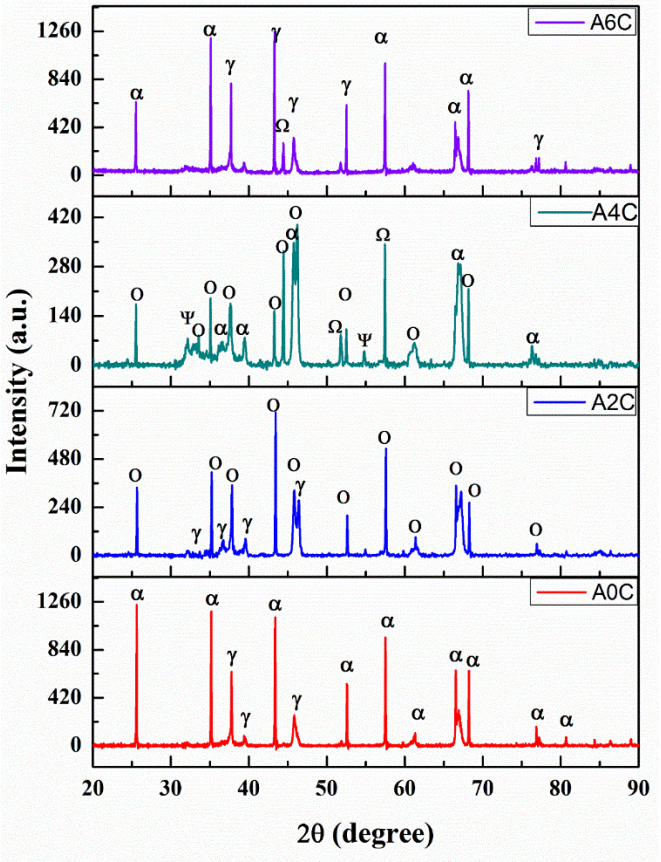

Figure 4.5 XRD pattern of the coatings fabricated with varying Alumina-chromia content.

In A2C, peaks corresponding to γ-Al_2O_3 and a significant number of O phase peaks ($Al_{1.98}Cr_{0.02}O_3$) appear. The presence of solid solution indicates initial Cr incorporation into the alumina lattice. Cr addition inhibits full transformation from γ to α phase, suggesting lattice distortion or stabilization of intermediate structures.

A4C contains all identified phases: α, γ, Ψ, Ω, and O. Formation of Cr_2O_3 and CrO phases indicates that Cr solubility in alumina matrix is exceeded, leading to precipitation of discrete Cr oxides. O peaks are still present, showing continued formation of Cr-substituted alumina. A6C coatings were dominated again by α and γ-Al_2O_3 phases, with weaker O, Ω, and γ peaks.

Reduction in Cr oxide phases (Ψ, Ω) suggests possible diffusion and redistribution of Cr at higher dopant levels. This pattern implies re-crystallization or improved thermal stability of alumina matrix, even at higher doping levels.

Chromium doping has a pronounced effect on the phase structure of alumina. At lower doping levels, Cr is incorporated into the alumina lattice, forming a solid solution ($Al_{1.98}Cr_{0.02}O_3$), while suppressing the transition from γ to α phase. At higher Cr levels, excess Cr forms separate oxide phases such as Cr_2O_3 and CrO. The complex interaction between alumina and Cr influences crystallinity, phase stability, and possibly the material's thermal and mechanical behavior.

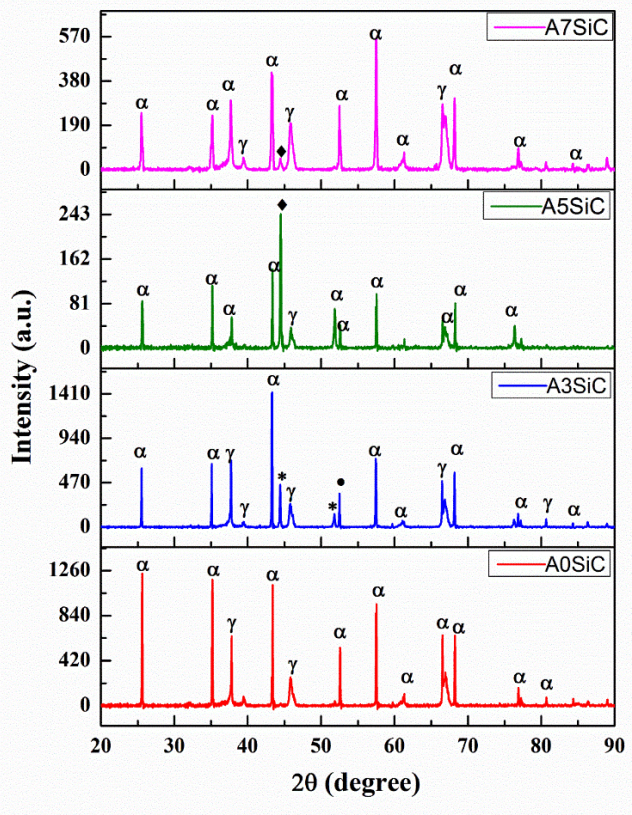

Figure 4.6 XRD pattern of the coatings fabricated with varying Alumina-SiC content.

XRD patterns of alumina-based composites with varying SiC content (A0SiC, A3SiC, A5SiC, and A7SiC) were analyzed to investigate phase evolution with SiC addition. The detected phases are indexed as follows:

α: α-Al_2O_3 (stable alumina)

γ: γ-Al_2O_3 (metastable alumina)

•: Si (elemental silicon)

★: C (carbon)

◆: SiC (silicon carbide)

In A0SiC (No SiC addition) Dominant peaks correspond to α-Al_2O_3, with sharp and intense signals indicating high crystallinity. Minor peaks of γ-Al_2O_3 show presence of a residual metastable phase, common in alumina sintering processes. No SiC peaks are observed, as expected.

In case of A3SiC, Presence of all major phases: α-Al_2O_3, γ-Al_2O_3, and minor peaks of Si (•), C (★), and SiC (◆). Detection of SiC confirms its formation due to the reaction between Si and C during sintering. Peaks for free Si and C suggest incomplete reaction or excess unreacted components. Overall, the phase structure is a multiphase composite with coexisting oxide, carbide, and elemental components. In A5SiC, α-Al_2O_3 remains the dominant phase, but peaks for γ-Al_2O_3 are weaker, indicating improved transformation to the stable phase. A clear SiC (◆) peak appears, showing enhanced SiC formation. No carbon or silicon peaks are detected, suggesting more complete reaction and phase incorporation compared to A3SiC. In A7SiC retains strong α-Al_2O_3 peaks along with visible γ-Al_2O_3 signals.

Distinct SiC (◆) peak remains, confirming SiC stability at high concentrations.
No unreacted Si or C observed, indicating effective conversion and good phase integration at this doping level.

The XRD analysis of SiC coatings demonstrates that SiC addition to alumina significantly alters the phase composition of the ceramic composite. Low SiC addition results in a multiphase structure with unreacted Si and C, while higher SiC contents (A5SiC and A7SiC) promote complete formation of SiC and more stabilized alumina phases. These results suggest enhanced phase compatibility and sintering behavior with increased SiC incorporation, potentially improving the mechanical and thermal properties of the composite.

4.5 Wear test analysis:

Table 4.2: Test conditions during linear reciprocating wear test

Counter body	Load (N)	Amplitude (mm)	Frequency (Hz)	Time (min)
WC-5wt.% CO (6 mm dia.)	10	2	12	15

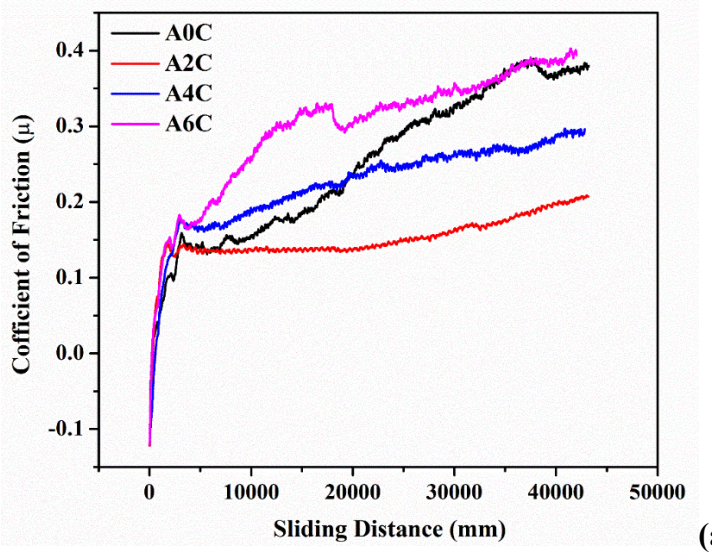

(a)

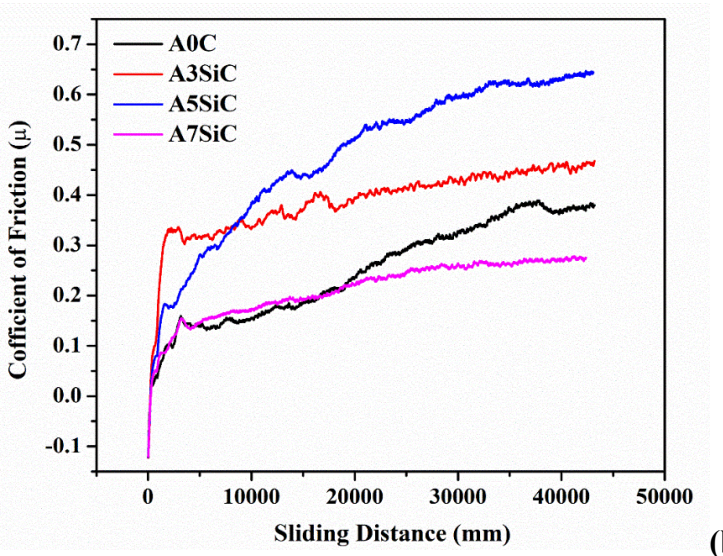

(b)

Figure 4.7 Variation of coefficient of friction with respect to sliding distance observed in different (a) Al_2O_3-Cr_2O_3 coatings and (b) Al_2O_3-SiC coatings

Figures 13(a) and 13(b) depict the evolution of the coefficient of friction as a function of sliding distance.

Alumina–Chromia Coatings [Fig.13 (a)]:

All coatings show a rise in COF with increasing sliding distance. The A2C coating exhibits the lowest and most stable COF (~0.2), while A6C shows a significant increase, peaking around 0.4. This suggests that controlled Cr_2O_3 content promotes a lubricating effect, whereas excess addition results in abrasive interaction.

Alumina–SiC Coatings [Fig. 13(b)], The COF behavior is more pronounced with SiC reinforcements.

A5SiC displays the highest COF (~0.65), possibly due e to increased micro-cutting effects. A7SiC surprisingly shows the lowest COF (~0.3), highlighting a beneficial role of SiC at higher concentrations in reducing interfacial shear.

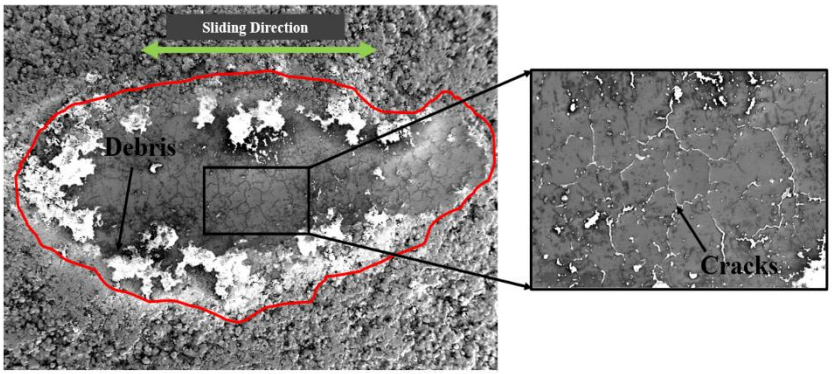

Figure 4.8 Wear track SEM image

The wear track morphology observed under SEM (Scanning Electron Microscopy) is shown in Figure [14]. The analysis provides insight into the wear mechanisms operative during dry sliding conditions of coated surfaces.

The left side of the figure illustrates a macroscopic wear track, where the sliding direction is clearly marked with a green arrow. The wear-affected zone is enclosed within a red boundary, revealing the overall extent of material degradation due to sliding. The zoomed-in microstructure on the right offers a microscopic view of the worn surface, enabling interpretation of microstructural damage.

The zoomed-in region on the right reveals significant plastic deformation, accompanied by intergranular and transgranular microcracking. These cracks are seen propagating along grain boundaries, indicating brittle fracture behavior in the coating during sliding.

The large white patches on the left side image within the red boundary signify delaminated regions. These areas appear to be coating fragments pulled out due to repeated contact stress, indicating adhesive wear. The central portion of the track (darker inner region) appears relatively smoother compared to the outer periphery. This suggests that the central zone underwent a steady wear regime with smoother material removal. The peripheral edges show accumulated debris and possible re-deposition, contributing to a rougher appearance. Within the smoother central region, there is evidence of tribolayer formation (compacted wear debris layer). This can act as a protective layer, temporarily reducing friction and wear but may break down under prolonged sliding. The elongated shape of the wear scar aligned along the sliding direction indicates directional wear, driven by the reciprocating or unidirectional motion during testing. The morphology also reflects the anisotropic response of the coating surface to the sliding motion.

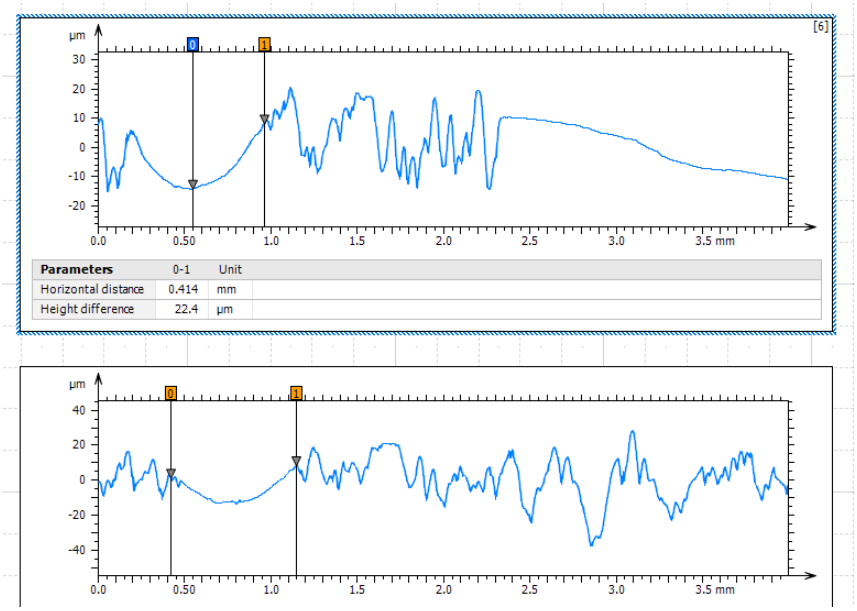

Figure 4.9 Wear track 2D profile

The provided image displays two 2D surface profiles of a wear track obtained via a contact-type profilometer. These profiles represent the surface topography across a wear track after tribological testing. The upper graph shows a 2D cross-sectional profile with notable features indicating wear. The profile clearly illustrates a groove-like depression in the surface, characteristic of abrasive or adhesive wear. This indicates a substantial depth of wear, with the groove depth reaching approximately 22.4 µm over a width of 414 µm. The central valley represents the main wear region, and the rising slopes on either side reflect the unworn or less worn surface. Surface roughness within and outside the wear track suggests material removal and possible debris adhesion. These 2D profiles are crucial for quantifying wear by providing the depth and width of the wear track.

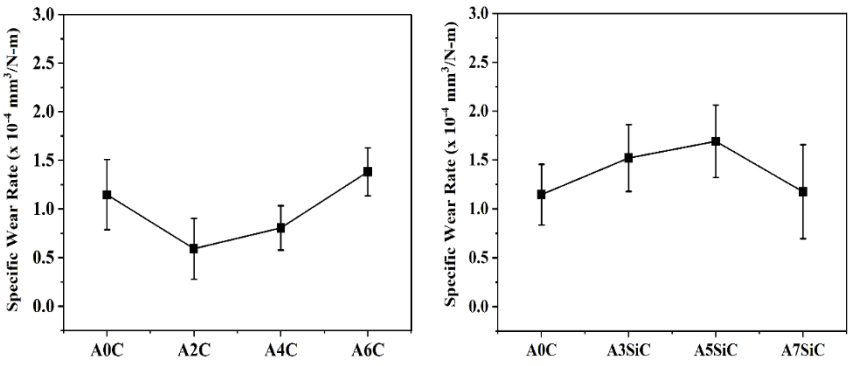

(a) **(b)**

Figure 4.10 Variation of specific wear rate with respect to wt. % in different (a) Al_2O_3-Cr_2O_3 coatings and (b) Al_2O_3-SiC coatings

Pure Al_2O_3, Al_2O_3-Cr_2O_3, and Al_2O_3-SiC coatings are subjected to sliding wear test (in a fretting wear tribometer) against a WC counterbody. The figure shows the variation of specific wear rate concerning Alumina wt. % chromia and SiC content. The tribological behavior of the fabricated coatings was assessed using wear testing, and the results were evaluated in terms of Specific Wear Rate (SWR) and Coefficient of Friction (COF). The comparative performance of Alumina–Chromia (A0C, A2C, A4C, A6C) and Alumina–Silicon Carbide (A0C, A3SiC, A5SiC, A7SiC) composites is presented and interpreted in this section. The figure illustrates the variation in specific wear rate of the coatings under dry sliding conditions.

In Alumina–Chromia coatings [Fig. 16(a)]; Pure alumina (A0C) exhibits a moderate wear rate. A2C demonstrates the lowest specific wear rate, indicating enhanced wear resistance due to optimal Cr_2O_3 reinforcement.
A further increase in chromia content (A4C, A6C) leads to increased wear, suggesting that excess Cr_2O_3 degrades mechanical integrity and accelerates wear.

Whereas in Alumina–SiC Coatings [Fig. 16(b)]; A similar trend is observed with SiC reinforcement. A5SiC shows the highest wear rate, despite a higher friction coefficient, indicating possible brittle behavior and surface degradation under sliding. Interestingly, A7SiC shows improved wear resistance over A5SiC, suggesting a threshold beyond which additional SiC stabilizes wear behavior. A2C's superior wear performance is attributed to the presence of fine Cr_2O_3 phases that strengthen the matrix without compromising toughness. Excess Cr_2O_3 in A6C introduces brittleness, leading to wear deterioration.

While in Alumina–SiC coatings SiC peaks (♦) are distinctly visible in A5SiC and A7SiC. A7SiC's improved friction and moderate wear are linked to a more refined and uniform SiC dispersion in the alumina matrix. The wear analysis demonstrates that controlled addition of reinforcements significantly affects the tribological performance of alumina-based coatings. Specifically:
A2C emerges as the most effective composition with the lowest wear and COF, attributed to optimized Cr_2O_3 dispersion. In contrast, excessive reinforcement (A6C, A5SiC) leads to poor wear

resistance, likely due to microstructural brittleness or phase incompatibility.

A7SiC, despite a higher reinforcement level, balances friction reduction and wear resistance, suggesting improved SiC dispersion at this concentration. These findings provide valuable insights into the design of wear-resistant ceramic coatings for engineering applications.

Conclusion

This study successfully demonstrated the deposition of alumina-based coatings with low additions of chromia (Cr_2O_3) and silicon carbide (SiC) using the flame spray technique. The investigation revealed significant insights into the microstructural evolution, phase composition, wear behavior, and porosity characteristics of the developed coatings.

X-ray diffraction (XRD) analysis confirmed the formation of a stable α-Al_2O_3 phase in all coatings, with the Al_2O_3–4 wt.% Cr_2O_3 variant showing the presence of a solid solution phase ($Al_{1.98}Cr_{0.02}O_3$), indicating effective Cr_2O_3 incorporation. In the SiC-added coatings, a higher SiC content (7 wt.%) further promoted the formation of stable α-Al_2O_3, highlighting its beneficial effect on phase stabilization.

In terms of tribological performance, the Al_2O_3–2 wt.% Cr_2O_3 coating exhibited the lowest coefficient of friction and the highest wear resistance among the Cr_2O_3-reinforced variants, making it the most effective formulation for wear-critical applications. Conversely, the Al_2O_3–7 wt.% SiC coating demonstrated inferior wear resistance, suggesting that excessive SiC may adversely affect the mechanical integrity of the coating. Porosity analysis indicated a decreasing trend with the initial addition of Cr_2O_3 (notably in A2C and A4C coatings), while further addition led to increased porosity (A6C). Interestingly, among SiC-containing coatings, the Al_2O_3–3

wt.% SiC coating exhibited the lowest porosity, implying an optimal reinforcement level for achieving a dense microstructure.

Overall, the findings underscore the potential of fine-tuning Cr_2O_3 and SiC additions to enhance specific properties of alumina-based coatings. The flame spray technique proved to be an effective and economical method for producing functional ceramic coatings with tailored performance characteristics suitable for wear-resistant applications.

REFERENCES

[1]. *Kang, J. J., et al. "Influence of spraying parameters on the microstructure and properties of plasma-sprayed Al2O3/40% TiO2 coating." Physics Procedia 50 (2013): 169-176.*

[2]. *Hauer, Michél, et al. "Use of Different Process Gases for Manufacturing Isolating Alumina Coatings by Flame Spraying with Cords." Journal of Thermal Spray Technology 30 (2021): 222-235.*

[3]. *Lampke, Thomas, et al. "Corrosion and wear behavior of alumina coatings obtained by various methods." Materials Science 46 (2011): 591-598.*

[4]. *Czupryński, Artur. "Flame spraying of aluminum coatings reinforced with particles of carbonaceous materials as an alternative for laser cladding technologies." Materials 12.21 (2019): 3467.*

[5] *Li, Chang-Jiu, Jiao Zou, Hui-Bin Huo, Jian-Tao Yao, and Guan-Jun Yang. "Microstructure and properties of porous abradable alumina coatings flame-sprayed with semi-molten particles." Journal of Thermal Spray Technology 25 (2016): 264-272.*

[6] *Dhakar, B., Chatterjee, S. and Sabiruddin, K., 2017. Influence of process parameters on the formation of phases and mechanical properties of plasma sprayed Al2O3–Cr2O3 coatings. Materials Research Innovations, 21(6), pp.367-376.*

[7] *Dhakar, B., Chatterjee, S. and Sabiruddin, K., 2017. Phase stabilization of plasma-sprayed alumina coatings by spraying mechanically blended alumina–chromia powders. Materials and Manufacturing Processes, 32(4), pp.355-364.*

[8]. Habib, K. A., et al. "Influence of Al 2 O 3 Particle Size on Microstructure, Mechanical Properties and Abrasive Wear Behavior of Flame-Sprayed and Remelted NiCrBSi Coatings." Journal of Materials Engineering and Performance 26 (2017): 1647-1656.

[9] *Suman, Setu, and Kazi Sabiruddin. "Behavior of free-standing atmospheric plasma sprayed Al2O3–Cr2O3 solid solution-based coatings under cyclic heating at 1000° C." Surface and Coatings Technology 490 (2024): 131180.*